Keyhole Estimation of an MIMO-OFDM Train-to-Wayside Communication System on Subway Tunnels

Juan Moreno, *Student Member, IEEE*, Leandro de Haro, *Member, IEEE*, Carlos Rodríguez, *Member, IEEE*, Luis Cuéllar, and José Manuel Riera, *Senior Member, IEEE*

***Abstract*—This letter presents a deep insight on a real implementation of a train-to-wayside radio on subway tunnels that makes use of a 2 × 2 multiple-input–multiple-output orthogonal frequency-division multiplexing (MIMO-OFDM) setup. The main purpose of this letter is to study in detail the keyhole phenomenon of an MIMO-OFDM train-to-wayside communication system on a tunnel. MIMO keyholes are studied in different tunnels sections, and capacity results are provided. Moreover, we introduce the first keyhole measurements on a railway tunnel. Finally, we follow a quantitative approach to estimate keyhole probabilities on each tunnel stretch and capacity outage curves.**

***Index Terms*—Keyholes, multiple-input–multiple-output (MIMO), orthogonal frequency-division multiplexing (OFDM), propagation, railways, subway tunnels, train-to-wayside communications.**

I. Introduction

INCREASINGLY, railway systems and in particular subways need broadband train-to-wayside communications systems for two main applications: driverless train-control systems and noncritical radio-based services like CCTV, customer information, etc. These technologies have strong requirements, and one of the most important of them is the need of full duplex communication between train and wayside, with large bandwidth requirements. Currently used narrowband radio systems (such as TETRA or GSM-R) cannot meet these requirements [1].

3GPP LTE has been proposed as the new standard for railway communications [2] and, as it is widely known, one of the key technologies of LTE is multiple-input–multiple-output (MIMO) [3]. Whether used with LTE or with other systems, MIMO is likely to be a suitable technology to provide large bandwidth in such a hostile environment as railway tunnels [4]. However, the propagation of radio waves in tunnels may cause undesirable effects related to MIMO, in particular keyholes. A keyhole happens when we have low spatial correlation and a low rank in the channel matrix [5], so it is a phenomenon that seriously decreases the performance of the whole system and needs to be carefully studied. In this letter, the performance of a multiple-input–multiple-output orthogonal frequency-division multiplexing (MIMO-OFDM) train-to-wayside communication system on subway tunnels is analyzed, with a particular focus on the presence of keyholes (following a quantitative approach to estimate keyhole probabilities).

The influence of the tunnel cross-section in radio propagation is well known [6], so we present results measured on many radically different tunnels built up with different constructive methods to study carefully its impact on MIMO performance and keyhole influence.

It is almost impossible to properly reference every contribution related to MIMO in tunnels. However, we need to mention the most important research work related to this topic: the pioneer paper on this field [7] that provided narrowband measurements with both antennas placed in the ground, like many others [8], [9]; simulations [10]; and broadband measurements [11], [12] but with no train involved.

As far as we know, there are no broadband train-to-wayside measurements that consider keyholes in tunnels. Thus, in this literature review, we can only mention the keyhole's theoretical background [5] and, closer to the main contributions of this letter, the measurements and an experimental procedure to estimate keyholes reported in [13].

This letter is organized as follows. Section II briefly covers the general architecture of the MIMO testbed employed in the measurement campaign and the channel estimation and keyhole estimation procedure. In Section III, we present the obtained results, and, finally in Section IV, conclusions are presented.

II. Setup and Parameter Estimation

A. Setup

To carry out these measurements we opted for a testbed already developed by some members of this group [14] that makes use of an implementation of both a DVB-T2 transmitter and a receiver. The reason of this choice was our need of OFDM (LTE's technology for the downlink), diversity, and the fact that we could work at 594 MHz (close to the lowest LTE bands and also valid for railway purposes). This testbed makes use of the frame structure of DVB-T2, but unlike DVB-T2 [which is multiple-input–single-output (MISO)] [15], it is 2 × 2 MIMO. Table I summarizes the main parameters of the MIMO testbed.

This work was supported by the Spanish Ministry of Education and Innovation (MICINN), the SICOMORO Project under Ref. TEC2011-28789-C02-01, and the Universidad Politecnica de Madrid under Grant CH/003/2011.

J. Moreno and C. Rodríguez are with the Engineering Department, Metro de Madrid, 28007 Madrid, Spain (e-mail: juan.moreno@metromadrid.es; carlos@metromadrid.es).

L. de Haro, L. Cuéllar, and J. M. Riera are with the ETSI Telecomunicación, Universidad Politécnica de Madrid (UPM), 28040 Madrid, Spain (e-mail: leandro@gr.ssr.upm.es; luiscn@gr.ssr.upm.es; jm.riera@upm.es).

Color versions of one or more of the figures in this letter are available online at http://ieeexplore.ieee.org.

Digital Object Identifier 10.1109/LAWP.2014.2356076

TABLE I
MAIN PARAMETERS OF THE MIMO TESTBED

Parameter	Symbol	Value
FFT mode	-	2K
Guard Interval	*GI*	1/8
Scattered pilot pattern		PP1
Modulation	-	64QAM
Sampling frequency	F_s	9.1429 MHz
Useful symbol time	T_u	$2048/F_s$=224 μs
Guard time	T_g	$T_s/8$=28 μs
Symbol time	T_s	252 μs
Bandwidth	*BW*	8 MHz
Data subcarriers	N_d	1878
Carrier spacing	Δf	4.26 KHz

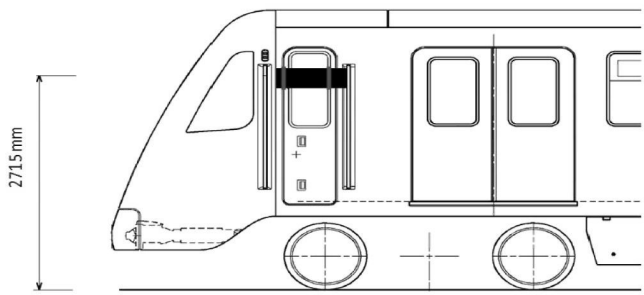

Fig. 1. Rolling stock of the 3000-2 series. The array was mounted on the cabin's window over a dielectric surface (in black).

In order to make the design and installation on the rolling stock simple, in this work we formed the arrays with short dipoles. All the antennas involved in these measurements are well matched at the desired frequency band. Fig. 1 shows the antenna array in one of the windows of the train. This location was chosen because most of the times it is impossible to place on-board antennas on the most suitable location (i.e., the front windshield), so we opted for a mid-suited easy-access location. Wayside antennas were placed at the end of the platform, the axis of the array 30° to the tunnel axis. This orientation was chosen to almost meet worst-case conditions. Antenna element spacing was λ (51 cm) on both arrays.

B. Channel Estimation

Here, we followed the same estimation procedure as in our previous paper [14], which is described in this section.

If $\boldsymbol{X_k}$ represents the transmitted data symbol vector (for the kth subcarrier), the received vector $\boldsymbol{Y_k}$ can be computed by

$$Y_k(t_l, f_k) = H_k(t_l, f_k)X_k(t_l, f_k) + N_k(t_l, f_k) \qquad (2)$$

where $\boldsymbol{H_k}$ is the MIMO channel matrix and $\boldsymbol{N_k}$ is the noise vector related to subcarrier k. Channel matrix normalization is shown in (3). It takes into account the average power of the OFDM symbol $\boldsymbol{H_k}$ (t_l, f_k) on every subcarrier of the symbol. Thus, for the lth symbol for every subcarrier k, we have the following channel matrix normalization:

$$h_{ij_{k,l}} = \frac{h_{ij}(t_l, f_k)}{\|H_k(t_l, f_k)\|}. \qquad (3)$$

This normalization decouples attenuation and channel-matrix properties, so the capacity (and the keyhole probability) is independent from the distance between transmitter and receiver (but not from other parameters, as, for example, tunnel cross section).

If we suppose equal (or uniform) power allocation for each subchannel, capacity can be computed using the classical equation for MIMO

$$C_{\mathrm{UP}} = \log_2\left[\det\left(I_M + \frac{\mathrm{SNR}}{N}HH^H\right)\right] \qquad (4)$$

where $\boldsymbol{M}$ and $\boldsymbol{N}$ are the number of receiving and transmitting antenna elements, respectively, and $\boldsymbol{H^H}$ means the transpose conjugate of $\boldsymbol{H}$. We compute $\boldsymbol{C_{\mathrm{UP}}}$ for each time $\boldsymbol{t_l}$ and subcarrier $\boldsymbol{f_k}$ (1878 subcarriers).

C. Keyhole Estimation

Tunnels can be considered oversized waveguides (cross-section dimension larger that λ), so we can assume that several modes are excited within the tunnel. Each one of them will have its own attenuation figures, so the combination of them at a single point could lead to fast fading conditions. These conditions are likely to help MIMO systems to improve its performance. This is the theoretical basis (from the modal point of view) of MIMO systems in tunnels [16].

On a diversity scenario, we know that, speaking in general, the higher the correlation of the signals, the lower the capacity of the channel. When we have a low spatial correlation between antennas and, unexpectedly, $\mathbf{H}$ has a low rank (ideally equal to 1), we may have a keyhole [5]. The example that better illustrates this scenario is a wall with a narrow hole on it separating the transmitting array and the receiving array. The mathematical formulation of this phenomenon can be obtained in the classic paper previously referred to [5].

To compute keyholes, we need to perform the singular value decomposition of $\mathbf{H_k}$. Hence, if $\mathbf{H} = UDV^H$, where $\boldsymbol{U}$ and $\boldsymbol{V}$ are unitary matrices and $\boldsymbol{D}$ is a diagonal matrix, whose elements are the nonzero eigenvalues of $\boldsymbol{H}$

$$D = \mathrm{diag}\left(\sqrt{\lambda_1}, \sqrt{\lambda_2}, \cdots \sqrt{\lambda_n}, 0, \cdots, 0\right). \qquad (5)$$

In our 2 × 2 MIMO scenario, we can have two eigenvalues at most ($\lambda_k = 0$ if $k > 2$). Then, to determine if we are under keyhole conditions, for each realization of $\mathbf{H_k}$, we follow the criterion of [13], as in

$$\frac{\max(\lambda_1,\lambda_2)}{\min(\lambda_1,\lambda_2)} = \left\{\begin{array}{ll} > SNR & \rightarrow \text{keyhole} \\ \leq SNR & \rightarrow \text{no keyhole} \end{array}\right\}. \qquad (6)$$

If we were in an ideal scenario (no noise) it would be enough to compute the rank of $\boldsymbol{H}$, but in the presence of noise, this will be misleading [13]. The measured SNR is 20 dB.

Then, we need to separate the influence on channel capacity of the correlation between elements in the array and the keyholes. This was done by checking that when a realization of $\mathbf{H}$ was under "keyhole conditions" (6), the correlation was below 0.75. This value guarantees that the measured correlation between the elements of the array does not play an important role [17]. Potential keyholes with correlations higher than 0.75 were discarded.

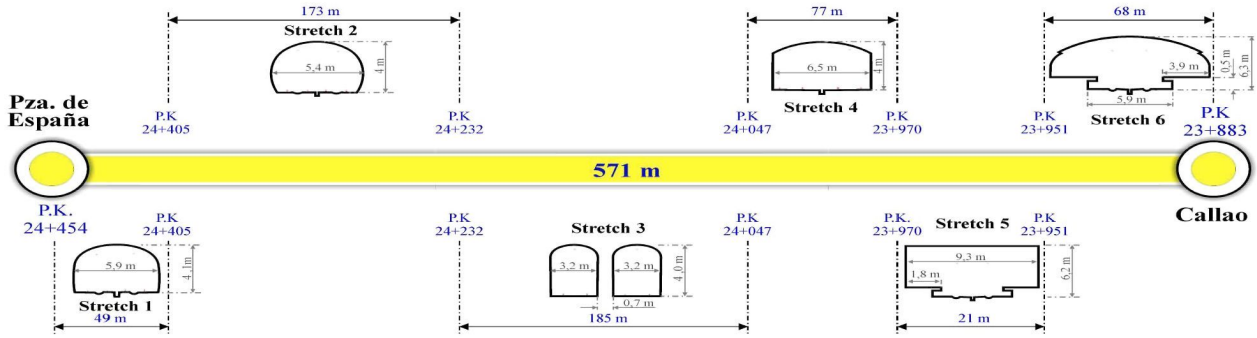

Fig. 2. Old tunnel cross sections (Callao–Plaza de España).

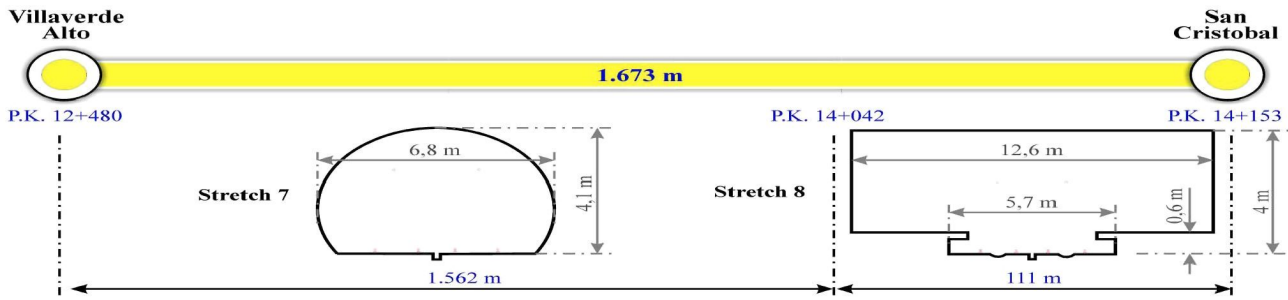

Fig. 3. New tunnel cross sections (Villaverde Alto–San Cristóbal).

III. Experimental Results

A. Measurements

We carried out a measurement campaign on Line 3 of Metro de Madrid. The measurements were performed on two different tunnels (Figs. 2 and 3), and for each scenario, 16 measurements were carried out. These two scenarios comprise a wide subway-tunnel variety: new and uniform tunnels, made by a boring machine, and the old ones, manually excavated with frequent changes on its cross section

The interstation Callao–Plaza de España is a 571-m shallow tunnel, and its cross section varies significantly in a short distance due to columns and other obstacles (see Fig. 2 for details of each stretch within this tunnel). On the other hand, the interstation of Fig. 3 is 1718 m long and was entirely carried through using a boring machine, so the cross section of the tunnel is very uniform.

The speed of the rolling stock is accurately fixed by the on-board signaling system, so we can guarantee that every measurement taken was carried out at the same speed (± 2 km/h). In our setup, as it is described in Section II, we placed both the on-board and the platform antenna in a realistic way that is somewhat far from the ideal conditions [18] for such a train-to-wayside setup.

B. Results

As we stated before, in this letter we provide two different results: MIMO capacity and keyhole statistics.

In Fig. 4, a summary of the conditional keyhole probabilities is provided. We see the probability of having a keyhole for each one of the six stretches that form the Callao–Plaza de España interstation (stretches 1–6, seen in Fig. 2) and two more stretches

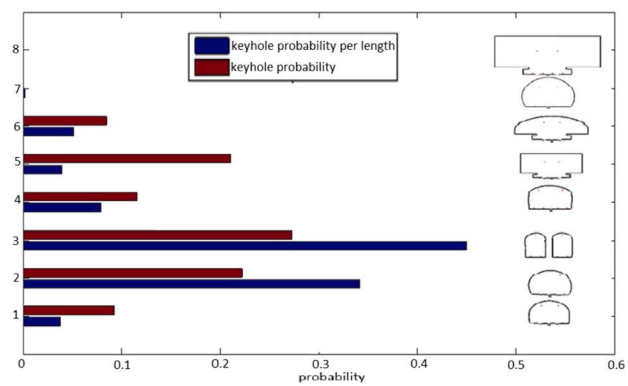

Fig. 4. Keyhole probabilities for each type of tunnel cross section. In blue, keyhole probability per meter; in red, keyhole probability with no normalization. At the right, we show the cross-section for each stretch. Stretches 1–6 belong to Fig. 2, and 7 and 8 to Fig. 3.

from the other tunnel (stretches 7 and 8, seen in Fig. 3). The higher the number of the stretch, the farther the transmitter and the receiver (1–6 on one side, and 7 and 8 on the other. See Figs. 2 and 3). We also provide a conditional keyhole probability taking into account the length of every stretch (in Fig. 4, in blue), and not only for the entire stretch (in Fig. 4, in red). We can see that the two-tubes stretch (Number 3, Fig. 2) concentrates almost 50% of keyholes, while its length only represents 32% of the measurement distance, even this stretch is not either the nearest or the farthest one. Tunnel stretch 7 is almost keyhole-free, and stretch 8 has no keyholes at all. Moreover, if we separately average every stretch of both old tunnel (stretches 1–6) and the new one (7 and 8), we find that it is far more likely to have a keyhole in the section-shifting old tunnel than in the "stable" new one. This is mostly due to the frequent

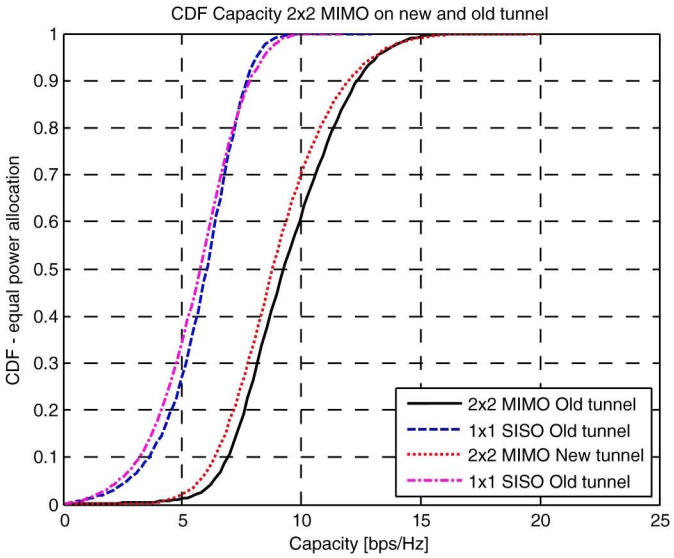

Fig. 5. Capacity CDF for old and new tunnel measurements. Antenna spacing between array elements is λ.

TABLE II
C_{90} VALUES FOR OLD AND NEW TUNNEL
[MIMO AND SINGLE-INPUT–SINGLE-OUTPUT (SISO)]

Tunnel	2x2 MIMO	1x1 SISO
Old tunnel	6.978	3.578
New tunnel	6.424	3.239

changes in the tunnel cross section and by the cross sections itself.

In Fig. 5, the obtained cumulative distribution function (CDF) for the capacity (measured in bits/second/Hertz) of the old and new tunnel scenarios are depicted. In order to extract further conclusions regarding the performance of the different MIMO configurations, a suitable parameter is the capacity exceeded in 90% of the measurements (C_{90}). See Table II for the C_{90} values.

If we compare the new tunnel and the old one in terms of capacity, we see that the capacity is better in the old tunnel. This is attributable to changes in tunnel cross section that led to a larger diversity (due to multipath because each change in the section implies that many modes are excited).

All these results clearly state that both changes in section and shape have a strong influence on keyhole probability. The stretch that concentrates more keyholes (per length unit) is stretch number 3, closely followed by number 2. Number 3 has many changes on its cross section due to the presence of columns between the two tubes. Stretches 7 and 8 have almost no irregularities of a significant size or cross-section changes and have almost no keyholes. Stretches 1 and 4 have similar shape and size and also have two very similar keyhole patterns. Thus, it is clearly stated that both changes in section and section itself have a strong influence on keyhole appearance.

IV. CONCLUSION

The performance of an MIMO-OFDM system has been evaluated with a measurement campaign carried out in the subway of Madrid, Spain. Keyhole probabilities have been estimated for many tunnel scenarios. Influence of tunnel cross section and changes in the cross section itself have a strong influence on the appearance of keyholes.

Somewhat paradoxically, tunnels more likely to have keyholes are also better in terms of capacity. The reason is that capacity is higher enough to overcome the decrement due to keyholes.

REFERENCES

[1] A. Bertout, "Changing track: Ground-to-train broadband communications and new train-borne applications are considering a move to 4G/LTE," 2009 [Online]. Available: http://www.railwaystrategies.co.uk
[2] UIC, "LTE/SAE—The future railway mobile radio system? Long-term visions on railway mobile radio technologies," V 0.4 Draft 14.09.2009, 2009.
[3] Q. Li *et al.*, "MIMO Techniques in WiMAX and LTE: A Feature Overview," *IEEE Commun. Mag.*, vol. 48, no. 5, pp. 86–92, May 2010.
[4] A. Goldsmith, S. Ali Jafar, N. Jindal, and S. Vishwanath, "Capacity limits of MIMO channels," *IEEE J. Sel. Areas Commun.*, vol. 21, no. 5, pp. 684–702, Jun. 2003.
[5] D. Chizik, G. Foschini, M. Grans, and R. Valenzuela, "Keyholes, correlations and capacities of multielement transmit and receive antennas," *IEEE Trans. Wireless Commun.*, vol. 1, no. 2, pp. 361–368, Apr. 2002.
[6] D. G. Dudley, M. Lienard, S. F. Mahmoud, and P. Degauque, "Wireless propagation in tunnels," *IEEE Antennas Propag. Mag.*, vol. 49, no. 2, pp. 11–26, Apr. 2007.
[7] M. Lienard, P. Degauque, J. Baudet, and D. Degardin, "Investigation on MIMO channels in subway tunnels," *IEEE J. Sel. Areas Commun.*, vol. 21, no. 3, pp. 332–339, Apr. 2003.
[8] J. Alonso Valdesueiro, B. Izquierdo, and J. Romeu, "On 2x2 MIMO observable capacity in subways tunnels at C-band: An experimental approach," *IEEE Antennas Wireless Propag. Lett.*, vol. 9, pp. 1099–1102, 2010.
[9] J. M. Molina-Garcia Pardo, M. Lienard, P. Degauque, C. Garcia-Pardo, and L. Juan-Llacer, "MIMO channel capacity with polarization diversity in arched tunnels," *IEEE Antennas Wireless Propag. Lett.*, vol. 8, pp. 1186–1189, 2009.
[10] Y. Cocheril, P. Combeau, M. Berbineau, and Y. Pousset, "MIMO propagation channel characteristics in tunnels," in *Proc. 7th Int. Conf. ITS Telecommun.*, 2007, pp. 1–6.
[11] C. Sanchís-Borrás, J. M. Molina-García Pardo, M. Lienard, and P. Degauque, "Performance evaluation of MIMO-OFDM in tunnels," *IEEE Antennas Wireless Propag. Lett.*, vol. 11, pp. 301–304, 2012.
[12] E. Masson *et al.*, "**4×4** MIMO channel sounding in tunnels for train-to-wayside communications," in *Proc. ICWCUCA*, Aug. 2012, p. 1.
[13] P. Almers, F. Tuvfesson, and A. F. Molisch, "Keyhole effect in MIMO wireless channels: Measurements and theory," *IEEE Trans Wireless Commun.*, vol. 5, no. 12, pp. 3596–3604, Dec. 2006.
[14] C. Gómez-Calero, L. Cuéllar, L. de Haro, and R. Martínez, "A 2x2 MIMO DVB-T2 system: Design, new channel estimation scheme and measurements with polarization diversity," *IEEE Trans Broadcast.*, vol. 56, no. 2, pp. 184–192, Jun. 2010.
[15] ETSI, Sophia-Antipolis, France, "Digital Video Broadcasting (DVB); Frame structure channel coding and modulation for a second generation Digital Terrestrial Television Broadcasting system (DVB-T2)," Draft ETSI EN 302 755 [1] V1.1.1 (2008-04), 2008.
[16] J. M. Molina-Garcia-Pardo, M. Liénard, P. Deqauque, and D. G. Dudley, "Interpretation of MIMO channel characteristics in rectangular tunnels from modal theory," *IEEE Trans. Veh. Technol.*, vol. 57, no. 3, pp. 1974–1979, May 2008.
[17] D. Shiu, J. G. Foschini, and J. G. Gans, "Fading correlation and its effects on the capacity of multielement antenna systems," *IEEE Trans. Commun.*, vol. 48, no. 3, pp. 502–513, Mar. 2000.
[18] Y. Cocheril, M. Berbineau, P. Combeau, and Y. Pousset, "On the importance of the MIMO channel correlation in underground railway tunnels," *J. Commun.*, vol. 4, pp. 224–231, May 2009.